

Pulsed Laser Copolymerization of Ring-Opening Cyclic Allylic Sulfide Monomers with Methyl Methacrylate and Styrene

Simon Harrisson and Thomas P. Davis*

Centre for Advanced Macromolecular Design, School of Chemical Engineering & Industrial Chemistry, University of New South Wales, Sydney, NSW 2052, Australia

Richard A. Evans and Ezio Rizzardo*

CSIRO Molecular Science, Clayton South, VIC 3169, Australia

Received July 6, 2001

ABSTRACT: Two cyclic allylic sulfide monomers, 6-methylene-2-methyl-1,4-dithiacycloheptane (MDTP) and 7-methylene-2-methyl-1,5-dithiacyclooctane (MDTO), were copolymerized with methyl methacrylate (MMA) using the pulsed laser polymerization technique. MDTO was also copolymerized with styrene (STY) under the same conditions. Reactivity ratios in bulk monomer at 25 °C, based on the terminal model, were determined from ¹H NMR analyses of the copolymers as $r_{\text{MDTP}} = 0.85$, $r_{\text{MMA}} = 11$ (MDTP–MMA); $r_{\text{MDTO}} = 1.22$, $r_{\text{MMA}} = 3.08$ (MDTO–MMA); and $r_{\text{MDTO}} = 0.3$, $r_{\text{STY}} = 8.6$ (MDTO–STY). The average propagation rate coefficients, $\langle k_p \rangle$, were determined for the copolymerizations in the monomer composition ranges $0 \leq f_{\text{MDTP}} \leq 0.6$ (MDTP–MMA), $0 \leq f_{\text{MDTO}} \leq 0.4$ (MDTO–MMA) and $0 \leq f_{\text{MDTO}} \leq 0.3$ (MDTO–STY). It was not possible to obtain values for $\langle k_p \rangle$ from mixtures containing higher mole fractions of MDTP or MDTO or for either homopolymer. The failure of pulsed laser polymerization in MDTP- and MDTO-rich solutions is presumably due to high rates of transfer to the cyclic allylic sulfide monomer. The MMA copolymerization data show clear deviation from the terminal model, similar to that observed by this group for 2-methylene-1,3-dioxepane. Significant solvent effects on the k_p of MMA were observed in the presence of 1,5-dithiacyclooctane, used as a nonpolymerizing model compound for MDTP and MDTO.

Introduction

Pulsed laser polymerization (PLP)¹ is firmly established as a tool for measuring propagation rate coefficients in free-radical polymerizations. The technique has been extended to measure average propagation rate coefficients, $\langle k_p \rangle$, in radical copolymerizations and terpolymerizations. In virtually all the systems that have been studied, the kinetics have deviated substantially from the predictions of the Mayo–Lewis terminal model.

To describe the kinetics that have been observed, a number of models have been proposed, of which the most widespread is the penultimate unit model, in either its implicit² or explicit³ forms. These models assume that both the penultimate and terminal units of the propagating radical affect the radical reactivity and have eight characteristic constants: the two homopropagation rates (k_{ii}), four monomer reactivity ratios (r_i and r'_i), and two radical reactivity ratios (s_i). These are defined as follows:

$$r_i = k_{iif}/k_{ijj} \quad (1)$$

$$r'_i = k_{jif}/k_{jjj} \quad (2)$$

$$s_i = k_{jii}/k_{iii} \quad (3)$$

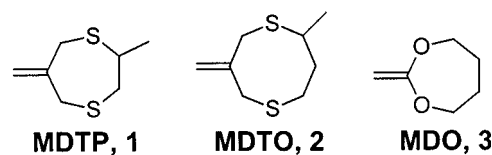
$$(i \neq j \text{ and } i, j = 1 \text{ or } 2)$$

The implicit penultimate unit model is a simplification of the explicit model that assumes $r_i = r'_i$.

It is difficult to discriminate between these two models due to the large number of variables contained

in each. However, there is evidence to indicate that the explicit model may provide a more satisfactory model of the elementary processes in radical copolymerization reactions.³

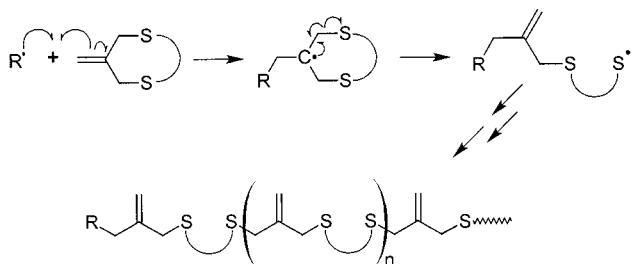
The “penultimate unit effect” is in reality a γ -substituent effect. Cyclic ring-opening monomers such as 6-methylene-2-methyl-1,4-dithiepane (MDTP, **1**), 7-methylene-2-methyl-1,5-dithiacyclooctane (MDTO, **2**) or 2-methylene-1,3-dioxepane (MDO, **3**) offer a potential means of simplifying the situation, as their propagating radicals are 7 or 8 atoms long, and hence have constant γ -substituents, even in copolymerizations. This should reduce the number of variables required to model the propagation reaction. Experiments performed on MDO,⁴ however, produced results that could not be modeled by the terminal model or either of the penultimate unit models.



MDTP and MDTO are cyclic allylic sulfide monomers.⁵ These compounds undergo 100% ring-opening free radical polymerization (Scheme 1) at or above room temperature to produce high-molecular-weight polymers.⁶ An unusual aspect of this polymerization is that the chain carrier is a sulfur-centered radical. This contrasts with most free-radical polymerizations in which the propagating radical is carbon-centered.

The work described in this paper is (to our knowledge) the first attempt to measure propagation rate coef-

* Corresponding authors: e-mail t.davis@unsw.edu.au, e.rizzardo@molsci.csiro.au.

Scheme 1. Mechanism of Polymerization of Cyclic Allylic Sulfide Monomers

ficients for ring-opening systems in which the chain carrier is a polymeric sulfur radical.

Experimental Section

Materials. The photoinitiators 2,2'-azobis(isobutyronitrile) (AIBN, obtained from BDH, 98%) and benzoin (BDH, 98%) were recrystallized twice from methanol. MMA (Aldrich, 99%) and STY (Aldrich, 99%) were passed through columns of basic alumina. MDTO was prepared according to the method described in reference.⁷ All monomers and initiators were stored in the dark under refrigeration.

SEC Analyses. Molecular weight distributions were determined by size exclusion chromatography using a GBC Instruments LC1120 HPLC pump, a Shimadzu SIL-10A autoinjector, a column set consisting of a Polymer Laboratories 3.0 μ m bead-size guard column (50 \times 7.5 mm) followed by four linear PL columns (10⁶, 10⁵, 10⁴, and 10³), and a VISCOTEK dual detector model 250 differential refractive index detector. Tetrahydrofuran (BDH, HPLC grade) was used as eluent at 1 mL/min. Calibration of the SEC equipment was performed with narrow polydispersity poly(methyl methacrylate) (PL, molecular weight range 200–1.6 \times 10⁶ g mol⁻¹) and polystyrene standards (PL, 1250–9.8 \times 10⁵ g mol⁻¹). Molecular weight distribution analysis of the samples was performed using PL software. Copolymers containing MMA were analyzed using MMA calibration, while MDTO–STY copolymers were analyzed using calibration for STY. These calibrations, while approximate, can be justified for the specific studies undertaken in this paper. This is discussed in a later section.

NMR Analyses. ¹³C (50 MHz) and ¹H NMR (200 MHz) spectra were recorded on a Bruker spectrometer at 25 °C using CDCl₃ (Cambridge Isotope Laboratories) as solvent.

Synthesis of MDTP. MDTP was synthesized according to the method of Evans⁶ from 1,2-propanedithiol and 3-chloro-2-chloromethylpropene. ¹H NMR: δ 1.26 (d, J = 7 Hz, 3H, CH₃), 2.72 (dd, J = ca. 9, J = ca. 15, 1H, CHH), 3.2 (m, 3H, CHH + CH), 3.41 (dd, J = ca. 5, J = 16, 2H, allylic CH₂), 4.79 (s, 2H, =CH₂) ppm. ¹³C NMR: δ 21.0 (CH₃) 36.3 and 38.9 (2 \times allylic CH₂), 45.9 (CH₂), 46.7 (CH), 110.4 (=CH₂), 148.3 ppm (C=CH₂).

Synthesis of 1,5-Dithiacyclooctane. 1,3-Propanedithiol (40.0 g, 0.370 mol dissolved in 80 mL of MeOH) and 1,3-dichloropropane (41.8 g, 0.370 mol dissolved in 80 mL of MeOH) were simultaneously added by syringe pump (5 mL/h for 16 h) to a refluxing solution of Na (17 g, 0.74 mol) in MeOH (1 L). The MeOH was then removed under reduced pressure, and 200 mL of water was added. The resulting mixture was extracted with CH₂Cl₂. The extracts were dried and distilled twice under vacuum, yielding 13.3 g (24.2%) of 1,5-dithiacyclooctane; bp 60 °C, 0.1 mmHg. ¹H NMR: δ 2.7–2.8 (m, 4H, –CH₂–), 2.8 (m, 8H, –CH₂S–). ¹³C NMR: δ 30.18 (–CH₂S–), 30.78 ppm (–CH₂–). Density (25 °C): 1.14 g mL⁻¹.

Pulsed Laser Copolymerizations. Details of the PLP technique may be found in the original paper by Olaj et al.¹ or in recent reviews.^{8,9} The experimental setup used in this work has been described in detail in a number of earlier publications by this group.^{4,10–12} The essential features of the system are a Continuum Surelite I-20 pulsed Nd:YAG laser with a harmonic generator (Surelite SLD-1 and SLT in series),

which is used to generate 355 nm UV laser radiation, and a wavelength separator (Surelite SSP-2), used to isolate the 355 nm beam. In a typical example, MMA (1.37 g, 13.7 mmol), MDTP (0.63 g, 3.93 mmol, $f_{\text{MDTP}} = 0.223$), and benzoin (3.12 mg, 14.5 μ mol) were charged to a 10 \times 60 mm reaction cell and degassed by sparging with N₂. The cell was sealed with a rubber septum and placed in a thermostated copper sample cell (25 °C), where it was allowed to equilibrate for several minutes before laser irradiation began. After irradiation (5 min at 12–15 mJ/pulse) was complete, the polymer was isolated by precipitation from methanol (20 mL) and dried under vacuum at 40 °C until constant weight was attained. Conversions were measured gravimetrically and were less than 5% in all cases. Details of all pulsed laser copolymerization experiments are shown in Table 1.

Results

Copolymer Composition. Copolymers were prepared from different monomer feed compositions using pulsed-laser polymerization (see following section), and each polymer was analyzed by ¹H NMR to determine its composition. This was achieved for MMA–MDTP and MMA–MDTO copolymers by comparing the areas of the resonance at 3.6 ppm corresponding to [C(O)–OCH₃] of MMA repeat units (3 H) to the resonance at 4.75–5.05 ppm corresponding to the vinylidene [CH₂=C] group of the MDTP or MDTO repeat unit (2 H). The composition of STY–MDTO copolymers was determined by comparing the area of the aromatic resonance of the polystyrene repeat unit (6.2–7.4 ppm, 5 H) and the vinylidene MDTO resonance (4.5–5.05 ppm). The terminal copolymer composition equation was fitted to the composition data by nonlinear regression using the Contour program.¹³ This procedure produced estimates for the terminal reactivity ratios, r_1 and r_2 , shown in Table 2.

Utilizing the terminal model for calculating r values has limitations as the terminal model is approximate; it fails to account for penultimate unit effects, solvent effects, reversible cross-propagation,¹⁴ and ceiling temperatures. However, as recently discussed,¹⁵ it is a useful procedure to facilitate comparison with other copolymerization reactions previously reported in the literature. Copolymer composition plots for the three copolymers may be found in Figure S1 of the Supporting Information.

Pulsed-Laser Polymerization. Propagation rate coefficients, k_p (in homopolymerizations), and average propagation rate coefficients, $\langle k_p \rangle$ (copolymerizations), were determined using eq 4,¹

$$\nu = \langle k_p \rangle [M] t_f \quad (4)$$

where ν is the chain length generated between two consecutive pulses (obtained from the inflection points of the primary peak of the linear scale molecular weight distributions), $[M]$ is the monomer concentration, and t_f is the dark time between pulses. This expression is also valid for ring-opening polymerizations provided that the ring-opening step is rapid with respect to the propagation step. In the case of cyclic allylic sulfides, this assumption may be justified by the results of studies on radical reactions of related allylic sulfides,^{16–19} which have shown that β -scission occurs rapidly upon addition to the double bond.

If the assumption of relatively rapid ring-opening is incorrect, the apparent rate of propagation (in homopolymerization of a ring-opening monomer) will contain a contribution from the rate of the ring-opening

Table 1. Experimental Data for the PLP Experiments (25 °C)

M ₁ ^a	M ₂ ^a	[M ₁] (mol/L)	[M ₂] (mol/L)	f ₁ ^b	initiator (I)	[I] (mmol/L)	F ₁ ^c	t _f (s) ^d	time (min) ^e	M _{inf} ^f	⟨k _p ⟩ ^g (L/(mol s))
MDTP	MMA	0.00	9.35	0	AIBN	6.59	0	0.05	5	15 922	340
MDTP	MMA	0.00	9.35	0	AIBN	4.49	0	0.1	10	30 339	324
MDTP	MMA	1.03	8.00	0.114	benzoin	7.20	0.012	0.05	5	15 703	343
MDTP	MMA	1.12	7.88	0.124	AIBN	8.47	0.016	0.05	5	15 812	352
MDTP	MMA	1.24	7.71	0.139	AIBN	6.37	0.018	0.1	10	29 648	332
MDTP	MMA	1.94	6.78	0.223	benzoin	7.28	0.031	0.05	5	15 310	337
MDTP	MMA	2.13	6.53	0.246	AIBN	10.11	0.030	0.05	5	15 171	351
MDTP	MMA	2.14	6.52	0.247	AIBN	4.76	0.034	0.1	10	27 416	317
MDTP	MMA	2.78	5.65	0.330	benzoin	8.32	0.050	0.05	5	14 825	340
MDTP	MMA	2.87	5.54	0.341	AIBN	5.97	0.048	0.1	10	25 763	306
MDTP	MMA	3.24	5.03	0.392	AIBN	5.35	0.039	0.05	5	13 964	340
MDTP	MMA	3.39	4.83	0.412	AIBN	5.81	0.050	0.1	10	25 177	307
MDTP	MMA	3.49	4.69	0.427	benzoin	6.82	0.079	0.05	5	14 321	334
MDTP	MMA	4.28	3.62	0.542	benzoin	6.35	0.109	0.05	5	14 825	355
MDTP	MMA	4.59	3.20	0.589	AIBN	13.02	0.243	0.05	5	14 689	341
MDTP	MMA	5.34	2.17	0.711	benzoin	6.57	0.326	0.1	10	10 965	
MDTP	MMA	5.35	2.16	0.712	benzoin	5.67	0.330	0.05	5	8 414	
MDTP		6.91	0.00	1.000	AIBN	24.5	1.000	0.1	10	26 730	251
MDTP	—	6.91	0.00	1.000	benzoin	5.44	1.000	0.05	5	19 952	330
MDTO	MMA	0.00	9.35	0.000	AIBN	5.7	0.000	0.05	5	15 204	329
MDTO	MMA	0.00	9.35	0.000	benzoin	5.3	0.000	0.05	5	13 932	295
MDTO	MMA	0.00	9.35	0.000	AIBN	6.2	0.000	0.1	10	29 824	323
MDTO	MMA	0.00	9.35	0.000	benzoin	5.7	0.000	0.1	10	27 227	286
MDTO	MMA	0.91	7.88	0.112	AIBN	5.8	0.050	0.05	5	16 140	352
MDTO	MMA	0.93	7.86	0.114	benzoin	4.6	0.080	0.05	5	15 812	333
MDTO	MMA	0.95	7.83	0.116	AIBN	6.5	0.049	0.1	10	29 005	329
MDTO	MMA	1.63	6.74	0.208	AIBN	7.1	0.078	0.1	10	30 526	343
MDTO	MMA	1.72	6.59	0.221	AIBN	5.9	0.090	0.05	5	16 081	349
MDTO	MMA	2.08	6.01	0.273	AIBN	6.7	0.100	0.1	10	31 871	362
MDTO	MMA	2.14	5.90	0.283	AIBN	6.1	0.115	0.05	5	16 374	374
MDTO	MMA	2.40	5.49	0.322	benzoin	6.2	0.189	0.1	10	30 200	322
MDTO	MMA	2.41	5.47	0.324	benzoin	5.2	0.193	0.05	5	17 179	369
MDTO	MMA	2.64	5.10	0.360	benzoin	6.7	0.245	0.05	5	20 370	415
MDTO	MMA	3.63	3.49	0.531	benzoin	5.9	0.378	0.05	7	16 144	
MDTO	MMA	3.65	3.46	0.534	benzoin	5.9	0.379	0.1	10	18 197	
MDTO	MMA	3.66	3.44	0.536	benzoin	26.5	0.387	0.05	5	21 762	
MDTO	MMA	3.76	3.29	0.554	benzoin	131.5	0.446	0.05	5	20 276	
MDTO	MMA	4.56	1.98	0.715	benzoin	6.0	0.826	0.05	7	22 336	
MDTO	MMA	4.57	1.96	0.717	benzoin	6.0	0.649	0.1	10	18 239	
MDTO		5.77	0.00	1.000	benzoin	5.2	1.000	0.05	30	53 703	951
MDTO		5.77	0.00	1.000	benzoin	4.1	1.000	0.05	30	52 481	959
MDTO		5.77	0.00	1.000	benzoin	0.42	1.000	0.05	90	50 119	916
MDTO		5.77	0.00	1.000	benzoin	0.046	1.000	0.05	270	57 544	1052
MDTO	STY	0.00	8.73	0.000	AIBN	5.8	0.000	0.25	80	20 000	88
MDTO	STY	0.00	8.73	0.000	AIBN	6.8	0.000	0.10	40	8 472	92
MDTO	STY	0.49	8.01	0.062	AIBN	5.6	0.007	0.25	80	19 166	86
MDTO	STY	0.52	7.95	0.067	AIBN	7.3	0.010	0.10	40	8 222	92
MDTO	STY	0.95	7.31	0.124	AIBN	7.4	0.021	0.25	80	18 055	82
MDTO	STY	1.02	7.21	0.133	AIBN	7.0	0.018	0.10	40	7 333	88
MDTO	STY	1.56	6.41	0.209	AIBN	7.1	0.027	0.25	80	15 666	73
MDTO	STY	1.49	6.51	0.199	AIBN	5.6	0.030	0.10	40	6 944	80
MDTO	STY	1.56	6.40	0.210	AIBN	4.6	0.025	0.25	80	15 789	75
MDTO	STY	2.20	5.44	0.305	AIBN	7.7	0.050	0.10	40	5 614	75
MDTO	STY	2.73	4.64	0.390	AIBN	7.3	0.042	0.25	80	2 836	
MDTO	STY	2.67	4.73	0.380	AIBN	7.2	0.039	0.10	40	2 192	
MDTO	STY	3.22	3.89	0.474	AIBN	7.4	0.086	0.25	80	1 988	
MDTO	STY	3.41	3.62	0.506	AIBN	7.3	0.099	0.10	40	1 696	
MDTO	STY	3.82	2.99	0.581	AIBN	8.4	0.128	0.10	40	1 520	
MDTO	STY	4.60	1.80	0.735	AIBN	8.3	0.305	0.25	80	599	
MDTO	STY	4.21	2.39	0.657	AIBN	8.3	0.217	0.10	40	1 023	

^a M₁, M₂: monomers used (MDTP: 6-methylene-2-methyl-1,4-dithiepane; MMA: methyl methacrylate; MDTO: 7-methylene-2-methyl-1,5-dithiacyclooctane; STY: styrene). ^b f₁: feed ratio of M₁. ^c F₁: mole fraction of M₁ in the copolymer, obtained from ¹H NMR measurements, as described in the text. ^d Interpulse delay. ^e Total reaction time. ^f Molecular weight of the low-molecular-weight point of inflection. ^g Figures in italics represent approximate k_p values obtained from the points of inflection of molecular weight distributions that do not show PLP characteristics; these were used as lower limits to the actual k_p for modeling purposes (see text).

reaction, k_β. Under PLP conditions, the kinetic chain length will be given by eq 5.

$$\nu = \frac{1}{\frac{1}{k_p} + \frac{[M]}{k_\beta}} [M] t_f \quad (5)$$

In this equation, 1/(1/k_p + [M]/k_β) is equivalent to k_p in eq 4 and represents an overall rate coefficient of

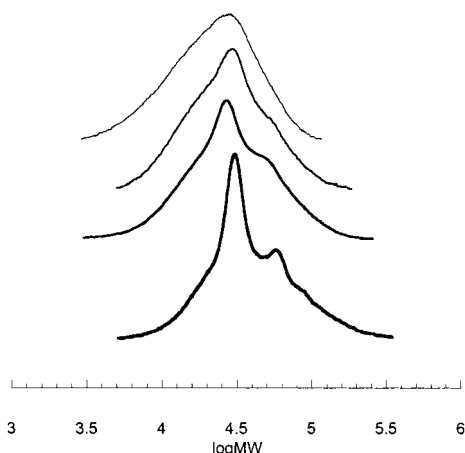
propagation. Use of eq 4 to represent such a system will lead to an apparent k_p which is dependent on the monomer concentration.

Polymer molecular weights were determined using size exclusion chromatography calibrated with MMA (for MMA copolymers) or STY (for the MDTO–STY copolymer) standards. The use of MMA or STY calibration is justified by the low level of cyclic allylic sulfide incorporation in the copolymer in the monomer feed ratios of interest.

Table 2. Terminal Model Reactivity Ratios (r_i , $i = 1, 2$) of Cyclic Allylic Sulfide Monomers with MMA and STY at 25 °C

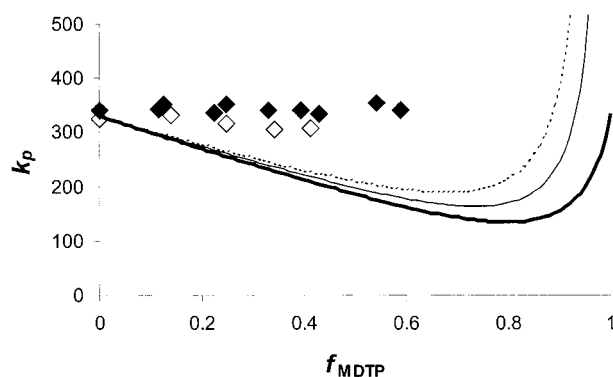
M_1^a	M_2^a	r_1	r_2
MDTP	MMA	0.85	11
MDTO	MMA	1.22	3.08
MDTO	STY	0.3	8.6

^a M_1 , M_2 : monomers used (MDTP: 6-methylene-2-methyl-1,4-dithiepane; MMA: methyl methacrylate; MDTO: 7-methylene-2-methyl-1,5-dithiacyclooctane; STY: styrene).

**Figure 1.** Sample polymer molecular weight distributions obtained from PLP experiments on MDTP–MMA at 25 °C, pulsing frequency 10 Hz. From bottom to top, the mole fractions of MDTP in the comonomer mixture are 0, 0.3, 0.5, and 0.7.

As the concentration of cyclic allylic sulfide in the comonomer mixture was increased, the polymer molecular weight distributions became broader, and PLP characteristics such as distinct overtones diminished (Figure 1). At 70 mol % MDTP, PLP characteristics had entirely disappeared. In MDTO copolymerizations, PLP characteristics were only obtained when f_{MDTO} was less than or equal to 0.4 (MMA) or 0.3 (STY). Attempts to homopolymerize either cyclic allylic sulfide monomer by the PLP method also produced broad, unimodal molecular weight distributions. When the cyclic allylic sulfide monomer concentration was sufficiently low, however, reproducible values of $\langle k_p \rangle$ were obtained. These values were independent of the pulse frequency (10 and 20 Hz).

We believe that the failure of the PLP technique at high concentrations of cyclic allylic sulfide is due to interruptions to chain growth during the dark time. The most likely cause of chain stopping is by chain-transfer reactions involving the cyclic allylic sulfide monomers, each of which has four easy-to-abstraction allylic hydrogens. Relatively high transfer to monomer constants have previously been measured for MDTO, **2** ($C_M = 63 \times 10^{-4}$ at 40 °C).⁷ The $\langle k_p \rangle$ values obtained from the inflection points of the molecular weight distributions produced at high MDTP and MDTO concentrations may nevertheless represent lower bounds of the actual values, as the absence of a discernible peak corresponding to laser-pulse-induced termination implies that the rate of propagation is fast enough for chains to reach the observed molecular weight before the subsequent flash. Consequently, we propose that the values of 330 and 1000 L mol⁻¹ s⁻¹ are lower limits to the k_p at 25 °C of MDTP and MDTO, respectively. Because of the use of MMA calibration in the molecular weight determination, these values are no more than order-of-magni-

**Figure 2.** Experimental $\langle k_p \rangle$ data obtained from PLP experiments on MDTP–MMA mixtures. Solid diamonds represent data obtained at 20 Hz and open diamonds at 10 Hz. The solid lines represent the predictions of the terminal model, using k_p of MDTP equal to 330 L mol⁻¹ s⁻¹ (—) or 33 000 L mol⁻¹ s⁻¹ (—). The dotted line represents the implicit penultimate unit model predictions with k_p of MDTP equal to 33 000 L mol⁻¹ s⁻¹; $S_{\text{MMA}} = 5000$.

tude estimates and were used as such in subsequent modeling (see below).

MMA–MDTP. Figure 2 shows the measured $\langle k_p \rangle$ values for MDTP/MMA monomer mixtures at 25 °C. In the region $0 \leq f_{\text{MDTP}} \leq 0.5$, the values remain almost constant. The terminal model predicts, however, that the $\langle k_p \rangle$ value should fall significantly, due to the low reactivity of MMA toward MDTP. The solid lines in Figure 2 represent the predictions of the terminal model, using the experimentally determined reactivity ratios and k_p values for MDTP of 330 and 33 000 L mol⁻¹ s⁻¹. Regardless of the actual value of the rate coefficient of MDTP homopropagation, the terminal model cannot fit the observed data.

Attempts to fit an implicit penultimate unit model to these data also fail, as the length of the MDTP repeat unit precludes a penultimate unit effect on MDTP-type radicals, and any penultimate unit effect on MMA-type radicals will have little effect on the average propagation rate constant at low MDTP concentrations, which is where the discrepancy is observed. Even with unrealistic values of k_p for MDTP of 33 000 L mol⁻¹ s⁻¹ and S_{MMA} of 5000, the predicted values are much lower than the experimental data (Figure 2).

MMA–MDTO. Similar results are observed in the MDTO–MMA copolymerization. The $\langle k_p \rangle$ steadily increases in the range $0 \leq f_{\text{MDTO}} \leq 0.4$, beyond which point PLP characteristics are no longer observed. Meanwhile, the terminal propagation model predicts a slight decline in $\langle k_p \rangle$, due to the relatively low reactivity of MMA toward MDTO, regardless of the value used for k_p of MDTO. To produce $\langle k_p \rangle$ values that approach those observed, a penultimate unit effect on propagation of MMA of the order of 50 is required, combined with a large $k_{p,\text{MDTO}}$ of 10 000 L mol⁻¹ s⁻¹ (Figure 3). It is difficult to visualize how such a large effect might arise.

STY–MDTO. The final copolymer mixture studied in this series of experiments was STY–MDTO. Across the observable range of solution compositions ($0 \leq f_{\text{MDTO}} \leq 0.3$), the observed $\langle k_p \rangle$ decreases roughly proportionally to the feed concentration of STY. The terminal model prediction is relatively insensitive to the value of $k_{p,\text{MDTO}}$, giving virtually identical results for values of 1000 and 10 000 L mol⁻¹ s⁻¹ (Figure 4). Agreement between the terminal model predictions and experimental results is relatively good.

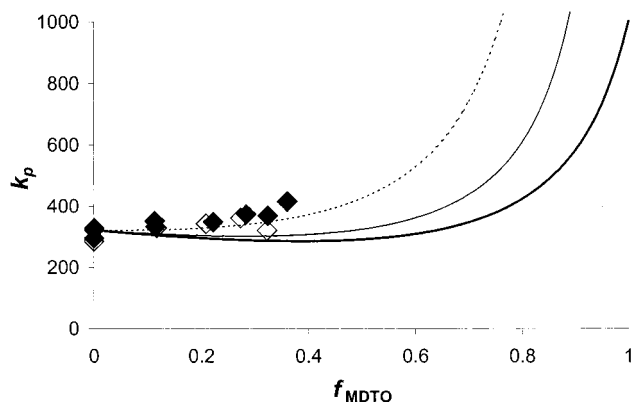


Figure 3. Experimental $\langle k_p \rangle$ data obtained from PLP experiments on MDTO–MMA mixtures. Solid diamonds represent data obtained at 20 Hz and open diamonds at 10 Hz. The solid lines represent the predictions of the terminal model, using k_p of MDTO equal to 1000 $\text{L mol}^{-1} \text{s}^{-1}$ (—) or 10 000 $\text{L mol}^{-1} \text{s}^{-1}$ (---). The dotted line represents the implicit penultimate unit model predictions with k_p of MDTO equal to 10 000 $\text{L mol}^{-1} \text{s}^{-1}$; $S_{\text{MMA}} = 50$.

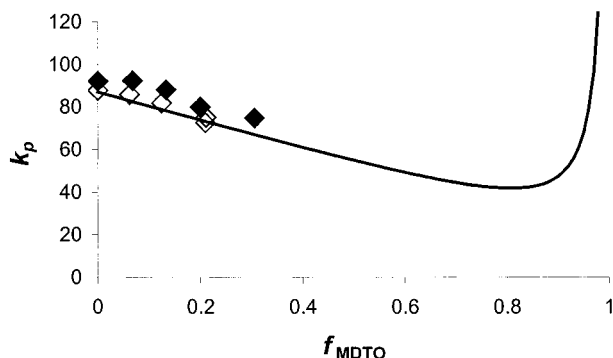


Figure 4. Experimental $\langle k_p \rangle$ data obtained from PLP experiments on MDTO–STY mixtures. Solid diamonds represent data obtained at 10 Hz and open diamonds at 4 Hz. The solid line represents the predictions of the terminal model, using k_p of MDTO equal to 1000 $\text{L mol}^{-1} \text{s}^{-1}$ (—). The use of higher values of $k_{p,\text{MDTO}}$ does not make a significant difference to the terminal model prediction in the region of interest ($f_{\text{MDTO}} = 0.3$).

The $\langle k_p \rangle$ data reported above are subject to some errors from the approximate GPC calibration. However, these errors are minimized as the data are obtained from copolymers that are rich in MMA or STY. The large discrepancy between the $\langle k_p \rangle$ data and the terminal/penultimate model predictions (for MMA copolymerizations) cannot be explained by small errors in GPC. (The STY–MDTO data that do conform to the terminal model are subject to a similar approximation.)

Interpretation of the Observed $\langle k_p \rangle$ Values. These observations accord with those recently made on the copolymerization of MMA with the cyclic ketene acetal, MDO (**3**),⁴ which also has $\langle k_p \rangle$ values that cannot be fitted by either terminal or penultimate unit models. It has been suggested⁴ that this behavior could be due to an extreme bootstrap effect or complex formation.

One obvious similarity between the monomers in this study and MDO is that they all polymerize via a ring-opening mechanism. This suggests that the mechanism of ring-opening may be connected with the unusual results observed. In the case of MDTP and MDO, however, the level of incorporation in the MMA copolymer is so low that the amount of ring opening is negligible compared to the MMA homopropagation

reaction. Furthermore, the incorporation of an extra step in the mechanism, however fast, could only decrease the observed value of $\langle k_p \rangle$. While the MDTO–MMA copolymerization can be fitted to the penultimate unit model (albeit using unrealistically large $k_{p,\text{MDTO}}$ and S_{MMA} values), it is likely that the acceleration of k_p in both MDTP and MDTO stems from the same cause, given their similar structures.

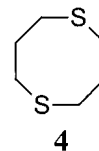
For similar reasons, the effect of reversible cross-propagation reactions, as observed in copolymerizations of MDTO,¹⁴ can also be discounted. While such reactions have a large effect on the copolymerization kinetics at low monomer concentrations, high temperatures, and high MDTO feed ratios, under the conditions of these experiments (bulk monomer, 25 °C and low f_{MDTO}) the kinetics should closely approximate the terminal model.

Hence, the effect must be due to solvent-type interactions between MMA radicals or MMA monomer and the cyclic comonomer, such as comonomer–radical or comonomer–MMA complexes, rather than any peculiarities related to the propagation mechanism of the ring-opening comonomers.

Solvent effects on k_p have been described in many homopolymerizations, particularly those of MMA and vinyl acetate.^{20–25} These have frequently been explained in terms of the formation of electron donor–acceptor complexes between the radical and the solvent.^{20–23} In a previous study,²⁵ several aromatic solvents produced an increase in the k_p of MMA compared to its bulk value. In addition, DMSO produced an increase of 63% over the bulk k_p at an MMA concentration of 2.8 M. By contrast, the effects of these solvents on STY tended to be small or nonexistent.

Similarly, in the case of the results presented here, significant deviations from the terminal model predictions are observed for $\langle k_p \rangle$ in MMA copolymerizations, but the STY copolymerization conforms to the terminal model, at least for $f_{\text{MDTO}} \leq 0.3$. Similar behavior occurs in the MDO–STY system,²⁶ in which MDO acts as an inert diluent, without any incorporation into the polymer or observable effect on the STY propagation rate constant. The presence of an effect with MMA but not STY strongly suggests that there is an interaction between MMA or its polymeric radical and compounds **1–3** that does not occur with STY.

As solvents **1–3** all contain groups that may be conducive to the formation of electron donor–acceptor complexes. Both of the sulfur-containing monomers contain two sulfur atoms in a 1,5-configuration on a ring. A similar compound, 1,5-dithiacyclooctane (**4**), undergoes one-electron oxidation to form a radical cation with relative ease, with the formation of a transannular three-electron bond between the two sulfurs.^{27–29} MDO contains an unusually electron-rich double bond, due to its two ether substituents. PolyMMA radical, on the other hand, has a high electron affinity, comparable to that of tetracyanoethylene and chloranil, which form charge-transfer complexes with typical solvents used in polymerizations.^{21,22}



Compounds **1–3** may act as electron donors in forming complexes with polyMMA radicals, with the result

Table 3. k_p Data for Polymerizations of MMA in Bulk and in Solution in 1,5-Dithiacyclooctane

[MMA] (M)	[AIBN] (mM)	t_f (s) ^a	time (min) ^b	M_{inf} ^c	k_p (L/(mol s))
9.35	5.9	0.1	10	31 333	335
9.35	5.9	0.2	10	58 479	312
7.09	5.1	0.05	5	14 223	401
7.15	4.6	0.1	7	26 242	367
7.26	4.8	0.2	14	52 000	357
4.19	4.7	0.05	30	11 220	535
4.19	5.4	0.1	30	<i>d</i>	<i>d</i>

^a Interpulse delay. ^b Total reaction time. ^c Molecular weight of the low-molecular-weight point of inflection. ^d This experiment produced unimodal polymer without PLP characteristics (see Figure 6).

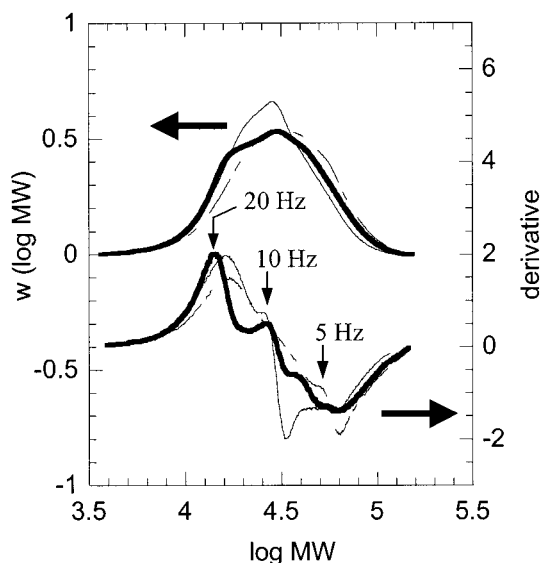
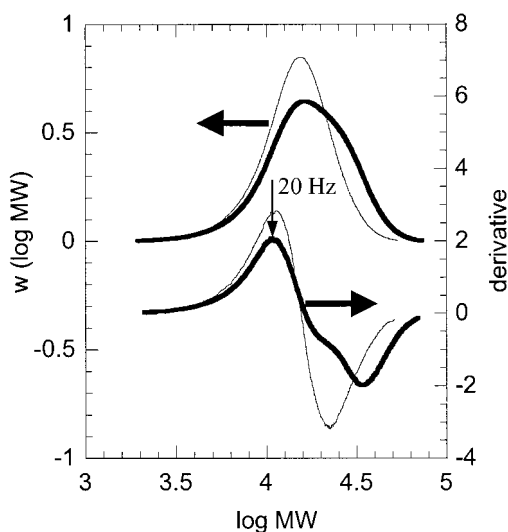
that the complexed radical has some anionic character. This in turn may increase the radical's reactivity toward the electron-deficient MMA double bond, in a manner analogous to the increased rates of cross-propagation observed in copolymerizations that tend to alternate, such as MMA–STY. The absence of a solvent effect in copolymerization with styrene may be explained by the electron-rich character of the polystyryl radical, which would make it less likely to act as the acceptor in a donor–acceptor complex with the comonomers.

Alternatively, compounds **1–3** may form donor–acceptor complexes with MMA monomer. Small variations in the IR spectra of MMA in solution in DMSO and liquid CO₂, possibly indicating the formation of solvent–monomer complexes, have been correlated with the change in k_p observed in these solvents.²⁴ Zammit et al. suggest,²⁵ on the basis of temperature-dependent measurements, that both solvent–radical and solvent–monomer complexes are important in determining the extent of the solvent effect, with solvent–radical complexes affecting the activation energy of k_p and solvent–monomer complexes affecting the preexponential term. Complexation can only lead to an increased propagation rate if the stabilization energy due to complexation of the reactants is more than compensated for by a similar stabilization of the transition state.⁴

Investigation of the cause of the effects observed in this study is complicated by the ability of **1–3** to copolymerize with MMA and would be much simplified by using a nonpolymerizable compound such as **4**. Preliminary results show that this compound does indeed appear to have a significant effect on the k_p of MMA.

Effect of 1,5-Dithiacyclooctane (4) on the k_p of MMA at 25 °C. The experimental k_p data obtained from MMA–**4** mixtures are shown in Table 3. At low MMA concentrations or slow flashing rates, chain transfer to **4** appears to be the dominant chain-stopping mechanism, preventing PLP analysis of the resulting molecular weight distributions.

The molecular weight distributions obtained at 20 mol % **4** ([MMA] = 7.2 M) are shown with their derivatives in Figure 5. While clear PLP characteristics are obtained at 20 Hz, it appears that at 10 Hz the lowest molecular weight point of inflection is in fact due to low molecular weight polymer formed by chain transfer, and the true primary PLP point of inflection is the second point, which is found at the same molecular weight as the second point of inflection of the 20 Hz sample. At 5 Hz, there is a small shoulder on the high molecular weight side of the molecular weight distribution, which has a point of inflection approximately 4 times that of the 20 Hz sample.

**Figure 5.** GPC-derived molecular weight distributions for PLP of MMA containing 20% 1,5-DTCCO. Flashing rates: (—) 20 Hz; (---) 10 Hz; (···) 5 Hz. Derivatives are shown below the MWDs. Arrows show the points used to obtain k_p data for Table 3.**Figure 6.** GPC-derived molecular weight distributions for PLP of MMA containing 50% 1,5-DTCCO. Flashing rates: (—) 20 Hz; (---) 10 Hz. Derivatives are shown below the MWDs. The arrow shows the point used to determine k_p data for Table 3.

At 50% **4**, PLP characteristics were only observed when a fast flashing rate of 20 Hz was used. Figure 6 shows molecular weight distributions obtained at 10 and 20 Hz. While the 20 Hz sample shows a clear point of inflection and a pronounced shoulder in the derivative trace at twice the molecular weight, the 10 Hz sample is unimodal and featureless. If both the point of inflection and the shoulder of the 20 Hz sample are presumed to be due to laser-induced termination, a k_p of 535 L mol⁻¹ s⁻¹ is obtained. Since the peak molecular weight is invariant between the two samples, it is possible that the first point of inflection is due to chain transfer, as for the 10 Hz sample at 20% **4**, and only the second point is a true “extra peak” due to PLP, leading to an estimated k_p of approximately 1000 L mol⁻¹ s⁻¹. In either case there is substantial solvent-induced acceleration of k_p .

Conclusions. The propagation kinetics of the MMA–MDTO and MMA–MDTP copolymerizations cannot be described by the terminal or penultimate unit models. The propagation kinetics of the STY–MDTO copolymerization, on the other hand, show no significant deviations from the terminal model in the monomer composition region that is accessible to the PLP technique ($f_{\text{MDTO}} \leq 0.3$, $T = 25\text{ }^{\circ}\text{C}$).

This behavior is similar to that of the cyclic ketene acetal MDO (**3**) in copolymerization with MMA⁴ or STY.²⁶ As the copolymers formed in all three MMA copolymerizations predominantly consist of MMA, we propose that the acceleration of $\langle k_p \rangle$ relative to the terminal and penultimate unit model predictions is predominantly due to solvent effects of the comonomer on the k_p of MMA. Such effects may occur through the formation of donor–acceptor complexes between the comonomers and either the polyMMA radical or MMA monomer, as both MDTO and MDTP contain sulfur atoms in 1,5-transannular positions, a functional group that is susceptible to one-electron oxidation,^{27–29} while MDO contains an unusually electron-rich ketene acetal double bond. Preliminary results on the PLP of MMA–1,5-dithiacyclooctane (**4**) mixtures show significant acceleration of k_p , appearing to confirm the involvement of the 1,5-transannular sulfurs.

Acknowledgment. We acknowledge funding from the Australian Research Council and an Australian Postgraduate Award to S.H. Help from Mr. Henry Yin in performing the PLP of 1,5-dithiacyclooctane–MMA mixtures is gratefully acknowledged.

Supporting Information Available: Figures showing the copolymer composition curves for MDTP–MMA, MDTO–MMA, and MDTO–STY copolymerizations. This material is available free of charge via the Internet at <http://pubs.acs.org>.

References and Notes

- (1) Olaj, O. F.; Bitai, L.; Hinkelmann, F. *Makromol. Chem.* **1987**, *188*, 1689.

- (2) Fukuda, T.; Ma, Y.-D.; Inagaki, H. *Makromol. Chem., Rapid Commun.* **1987**, *8*, 495.
- (3) Coote, M. L.; Davis, T. P. *Prog. Polym. Sci.* **1999**, *24*, 1217.
- (4) Roberts, G. E.; Coote, M. L.; Heuts, J. P. A.; Morris, L. M.; Davis, T. P. *Macromolecules* **1999**, *32*, 1332.
- (5) Evans, R. A.; Rizzardo, E. *Macromolecules* **1996**, *29*, 6983.
- (6) Evans, R. A.; Rizzardo, E. *J. Polym. Sci., Part A: Polym. Chem.* **2001**, *39*, 202.
- (7) Harrison, S.; Davis, T. P.; Evans, R. A.; Rizzardo, E. *Macromolecules* **2000**, *33*, 9553.
- (8) Coote, M. L.; Zammit, M. D.; Davis, T. P. *Trends Polym. Sci.* **1996**, *4*, 189.
- (9) van Herk, A. M. *J. Macromol. Sci., Rev. Macromol. Chem. Phys.* **1997**, *C37*, 663.
- (10) Morrison, D. A.; Davis, T. P. *Macromol. Chem. Phys.* **2000**, *201*, 2128.
- (11) Coote, M. L.; Davis, T. P. *Eur. Polym. J.* **2000**, *36*, 2423.
- (12) Coote, M. L.; Davis, T. P. *Macromolecules* **1999**, *32*, 4290.
- (13) *Contour*: van Herk, A. M. Available from the author: Laboratory of Polymer Chemistry, Eindhoven University of Technology, PO Box 513, 5600 MB Eindhoven, The Netherlands, 1996.
- (14) Harrison, S.; Davis, T. P.; Evans, R. A.; Rizzardo, E. *Macromolecules* **2001**, *34*, 3869.
- (15) Davis, T. P. *J. Polym. Sci., Part A: Polym. Chem.* **2001**, *39*, 597.
- (16) Meijs, G. F.; Rizzardo, E.; Thang, S. H. *Macromolecules* **1988**, *21*, 3122.
- (17) Meijs, G. F.; Rizzardo, E.; Thang, S. H. *Polym. Bull. (Berlin)* **1990**, *24*, 501.
- (18) Meijs, G. F.; Morton, T. C.; Rizzardo, E.; Thang, S. H. *Macromolecules* **1991**, *24*, 3689.
- (19) Barton, D. H. R.; Crich, D. *Tetrahedron Lett.* **1984**, *25*, 2787.
- (20) Kamachi, M. *Adv. Polym. Sci.* **1981**, *38*, 55.
- (21) Henrici-Olivé, G.; Olivé, S. *Z. Phys. Chem (Munich)* **1965**, *47*, 286.
- (22) Henrici-Olivé, G.; Olivé, S. *Makromol. Chem.* **1966**, *96*, 221.
- (23) Bamford, C. H.; Brumby, S. *Makromol. Chem.* **1967**, *105*, 122.
- (24) Beuermann, S.; Buback, M.; Schmaltz, C.; Kuchta, F.-D. *Macromol. Chem. Phys.* **1998**, *199*, 1209.
- (25) Zammit, M. D.; Davis, T. P.; Willett, G. D.; O'Driscoll, K. F. *J. Polym. Sci.: Polym. Chem.* **1997**, *35*, 2311.
- (26) Morris, L. PhD Thesis, UNSW, 2000.
- (27) Asmus, K.-D. *Acc. Chem. Res.* **1979**, *12*, 436.
- (28) Musker, W. K.; Wolford, T. L. *J. Am. Chem. Soc.* **1976**, *98*, 3055.
- (29) Musker, W. K.; Wolford, T. L.; Roush, P. B. *J. Am. Chem. Soc.* **1978**, *100*, 6416.

MA0111663